

Numerical Simulations of Reactive Flow Displacements in Porous Media

S. H. Hejazi and J. Azaiez[§]

Abstract— The viscous fingering of miscible flow displacements in a homogeneous porous media is examined in the case involving non-autocatalytic chemical reactions between the fluids. The problem is formulated using continuity equation, Darcy's law, and volume-averaged forms of convection-diffusion-reaction equation for mass balance. Full nonlinear simulations using a pseudo-spectral method, allowed to analyze the mechanisms of fingering instability that result from the dependence of the fluids viscosities on the concentrations of the different species. In particular, the study examined the effects of varying important parameters namely the Damkohler number that represents the ratio of the hydrodynamic and chemical characteristic time scales, and the Peclet number that accounts for the inertial versus diffusive effects.

Index Terms—Viscous fingering, miscible displacements, convection-diffusion-reaction, numerical simulations

I. INTRODUCTION

Flow displacements in porous media can result in an interfacial instability between the two fluids involved in the displacement process. This instability is manifested in the form of finger-shaped intrusions of the displacing fluid into the displaced one, hence it is referred to as the fingering or Saffman-Taylor instability [1]. When the instability is driven by a mismatch between the viscosities of the two fluids, it is referred to as the viscous fingering instability. There is a very rich literature on this instability that has focused on displacements in the absence of chemical reaction. For an extensive review of experimental and modeling studies one should consult [2-4].

Such instability may also develop in conjunction with chemical reactions in processes as varied as chromatographic separation, fixed bed regeneration, polymer synthesis and processing, oil recovery and oil-bearing treatment as well as flow induced spreading of chemical pollutants and their interaction with the environment. The subtle feedback between the flow dynamics and chemistry can result in hydrodynamic instabilities that are not observed in non reactive systems. There are a limited but growing number of experimental studies on reactive viscous fingering [5-10]. In

Manuscript received February 3, 2009. This work was supported in part by the Natural Science and Engineering Research Council of Canada (NSERC), the Alberta Ingenuity Center for In-Situ Energy (AICISE) and Alberta Ingenuity Fund (AIF).

S. H. Hejazi is with the University of Calgary, Department of Chemical and Petroleum Engineering (Phone: 1-403-220-5758; e-mail: shhejazi@ucalgary.ca).

J. Azaiez is with the University of Calgary, Department of Chemical and Petroleum Engineering (Phone: 1-403-220-7526; fax: 1-403-289-3452; e-mail: azaiez@ucalgary.ca).

these studies the effects of stoichiometry, medium orientation, external electrical field, chemical composition and interactions with surrounding porous media were investigated. There is an equally growing interest in modeling this reactive flow instability [11-23].

The vast majority of the above cited works on reactive flows dealt only with the buoyancy-driven Rayleigh-Taylor instability and focused on vertical tubes or Hele-Shaw cells or auto-catalytic reactions. Furthermore, the non-linear simulations were mainly focusing on auto-catalytic reactions. In the present study we propose to use numerical modeling to analyze the development of the instability in the presence of a chemical reaction where the two fluids involved in the displacement react and produce a third separate component.

II. MATHEMATICAL MODEL

A two-dimensional displacement is considered in which both fluids are incompressible and fully miscible. The flow is taking place in horizontal direction in a homogeneous medium of constant porosity ϕ and permeability k . A fluid (A) of viscosity μ_A is injected from the left-hand side with a uniform velocity U . This fluid displaces a second one (B) of viscosity μ_B . Here, the direction of the flow is along the x -axis and the y -axis is parallel to the initial plane of the interface. A chemical reaction occurs between the two fluids leading to the formation of a product (C) of viscosity μ_C :



A schematic of the two-dimensional porous medium/Hele-Shaw cell system is shown in Fig. 1.

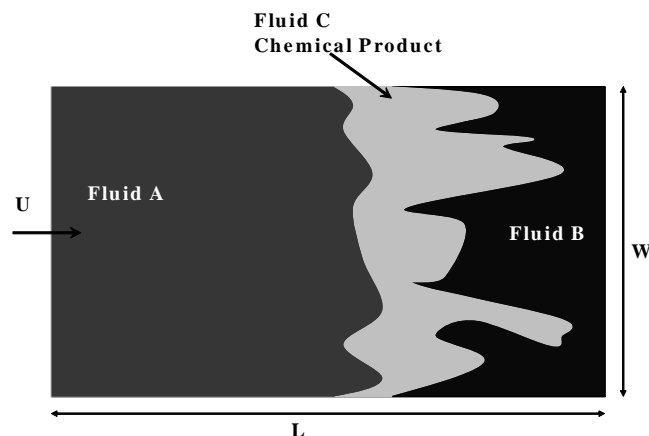


Fig.1. Schematic of rectilinear Hele-Shaw cell / two-dimensional porous medium.

The length, width and thickness (z -direction) of the

medium are L , W and b respectively. The governing equations are those for the conservation of mass, conservation of momentum in the form of Darcy's law and the convection-dispersion-reaction mass balance equation.

$$\nabla \cdot \mathbf{v} = 0 \quad (2)$$

$$\nabla p = -\frac{\mu}{K} \mathbf{v} \quad (3)$$

$$\frac{\partial A}{\partial t} + \frac{u}{\phi} \frac{\partial A}{\partial x} + \frac{v}{\phi} \frac{\partial A}{\partial y} = D_A \left(\frac{\partial^2 A}{\partial x^2} + \frac{\partial^2 A}{\partial y^2} \right) - kA.B \quad (4)$$

$$\frac{\partial B}{\partial t} + \frac{u}{\phi} \frac{\partial B}{\partial x} + \frac{v}{\phi} \frac{\partial B}{\partial y} = D_B \left(\frac{\partial^2 B}{\partial x^2} + \frac{\partial^2 B}{\partial y^2} \right) - kA.B \quad (5)$$

$$\frac{\partial C}{\partial t} + \frac{u}{\phi} \frac{\partial C}{\partial x} + \frac{v}{\phi} \frac{\partial C}{\partial y} = D_C \left(\frac{\partial^2 C}{\partial x^2} + \frac{\partial^2 C}{\partial y^2} \right) + kA.B \quad (6)$$

In the above equation, $\mathbf{v} = u\mathbf{i} + v\mathbf{j}$ is the velocity vector with u and v the x - and y - components respectively, p the pressure, μ the viscosity, k the reaction constant, K the medium permeability and ϕ its porosity. The concentrations of the two reactants and the product are denoted by A , B and C , respectively while D_A , D_B and D_C are their corresponding diffusion coefficients. In the present study, it will be assumed that all species have the same diffusion coefficient, i.e. $D_A = D_B = D_C = D$. Since the characteristic velocity for the fluid flow through the porous medium is U/ϕ , we adopted a Lagrangian reference frame moving at a velocity U/ϕ . Furthermore, diffusive time $D\phi^2/U^2$ and diffusive length $D\phi/U$ are chosen to make the length and time dimensionless. The constant permeability K is incorporated in the expression of the viscosity by treating μ/K as μ , and we shall refer to ratios of μ as either viscosity or mobility ratios. The rest of the scaling is as follows: the velocity is scaled with U/ϕ , the viscosity and pressure with μ_A and $\mu_A D\phi$, respectively, and the concentration with that of the pure displacing fluid, A_0 . The dimensionless equations are:

$$\nabla^* \cdot \mathbf{v}^* = 0 \quad (7)$$

$$\nabla^* p^* = -\mu^* (\mathbf{v}^* + \mathbf{i}) \quad (8)$$

$$\frac{\partial A^*}{\partial t^*} + \mathbf{u}^* \cdot \nabla^* A^* = \nabla^{*2} A^* - D_a A^* B^* \quad (9)$$

$$\frac{\partial B^*}{\partial t^*} + \mathbf{u}^* \cdot \nabla^* B^* = \nabla^{*2} B^* - D_a A^* B^* \quad (10)$$

$$\frac{\partial C^*}{\partial t^*} + \mathbf{u}^* \cdot \nabla^* C^* = \nabla^{*2} C^* + D_a A^* B^* \quad (11)$$

In the above equations, dimensionless variables are represented with asterisk while $D_a = kA_0 D/U^2$ is the

Damkohler number representing the ratio of hydrodynamic to chemical characteristic times. Two more dimensionless numbers are also involved, the Peclet number $Pe = UL/D$ and the cell aspect-ratio $A = L/W$ that appears in the boundary conditions [24]. To complete the model, a form for the dependence of the viscosity on concentration and temperature must be specified. Following previous studies, we assume that the viscosity varies exponentially with concentration [23-25],

$$\mu^* = \exp(R_b B + R_c C) \quad (12)$$

where R_b and R_c are the log-mobility ratios between the species as follows:

$$R_b = \ln\left(\frac{\mu_B}{\mu_A}\right) \quad \frac{R_c}{2} = \ln\left(\frac{\mu_C(C=0.5)}{\mu_A}\right) \quad (13)$$

For convenience, in all that follows, the asterisks will be dropped from all dimensionless variables.

III. NUMERICAL TECHNIQUE

The problem is formulated using a streamfunction-vorticity formulation, where the streamfunction ψ and the vorticity ω are related as:

$$\nabla^2 \psi = -\omega \quad (14)$$

where ∇^2 is the Laplacian operator. With the streamfunction-vorticity formulation, the continuity equation is satisfied automatically and the convection dispersion equations take the forms:

$$\frac{\partial A}{\partial t} + \frac{\partial \psi}{\partial y} \frac{\partial A}{\partial x} - \frac{\partial \psi}{\partial x} \frac{\partial A}{\partial y} = D_A \left(\frac{\partial^2 A}{\partial x^2} + \frac{\partial^2 A}{\partial y^2} \right) - kA.B \quad (15)$$

$$\frac{\partial B}{\partial t} + \frac{\partial \psi}{\partial y} \frac{\partial B}{\partial x} - \frac{\partial \psi}{\partial x} \frac{\partial B}{\partial y} = D_B \left(\frac{\partial^2 B}{\partial x^2} + \frac{\partial^2 B}{\partial y^2} \right) - kA.B \quad (16)$$

$$\frac{\partial C}{\partial t} + \frac{\partial \psi}{\partial y} \frac{\partial C}{\partial x} - \frac{\partial \psi}{\partial x} \frac{\partial C}{\partial y} = D_C \left(\frac{\partial^2 C}{\partial x^2} + \frac{\partial^2 C}{\partial y^2} \right) + kA.B \quad (17)$$

Taking the curl of equation (14) one gets:

$$\omega = R_b \left(\frac{\partial \psi}{\partial x} \frac{\partial B}{\partial x} + \frac{\partial \psi}{\partial y} \frac{\partial B}{\partial y} + \frac{\partial B}{\partial y} \right) + R_c \left(\frac{\partial \psi}{\partial x} \frac{\partial C}{\partial x} + \frac{\partial \psi}{\partial y} \frac{\partial C}{\partial y} + \frac{\partial C}{\partial y} \right) \quad (18)$$

Equations (14)-(17) form a closed set that can be solved for the concentration and velocity fields. Following the approach in [23] for auto-catalytic reactions, the system of partial differential equation is solved by decomposing the variables as a base-state and a perturbation. The perturbation terms consist of a random noise centered at the interface between A and B that decays rapidly in the stream-wise direction. The base-state, is a solution of the equations at a given short time t_0 . The resulting equations are solved using Hartley transform based pseudo-spectral method [26, 27].

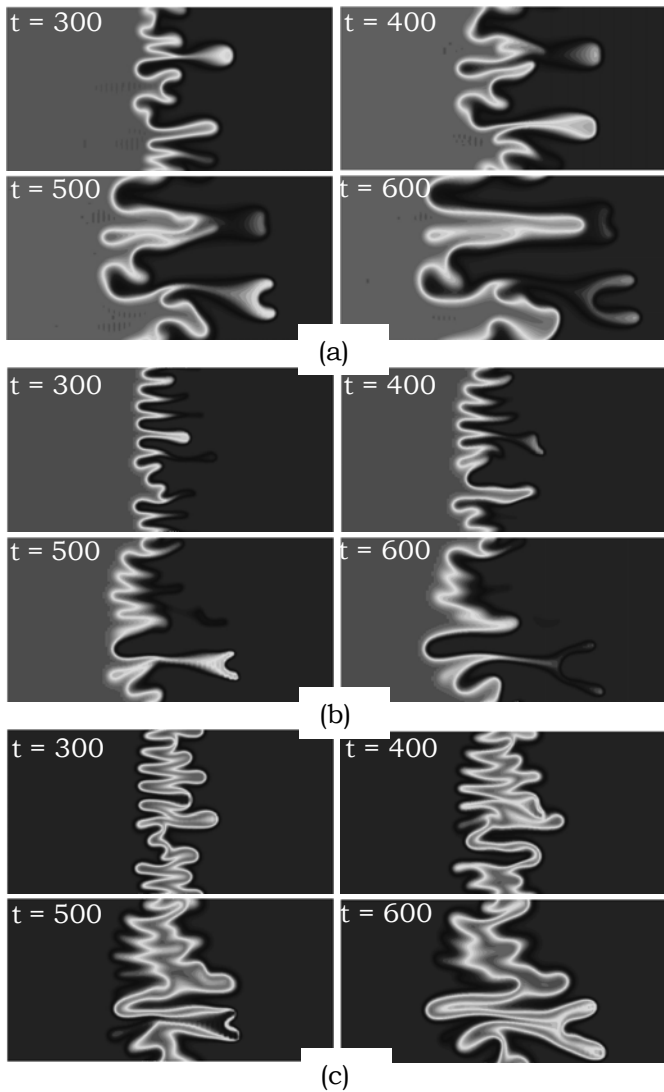


Fig 2. Concentration iso-surfaces for $Pe=1000$, $Rb=3$, $Rc=5$: (a) non-reactive system: $Da=0.0$, (b) reactive system: $Da=0.5$, reactant (A) iso-surfaces, (c) reactive system: $Da=0.5$, product (C) iso-surfaces

IV. RESULTS

The pseudo-spectral code has been validated first by simulating non-reactive cases that have already been published in the literature. It has been found that the time evolutions of the viscous fingers are identical to the results presented in [4]. Convergence of the numerical results has also been tested by varying the spatial resolution and the time steps. In what follows, results of the numerical simulations are presented for different values of the major dimensionless parameters that characterize the flow displacement.

In order to follow the nonlinear interactions of the fingers, time sequences of concentration iso-surfaces are presented for a fixed cell aspect ratio $A=2$. For brevity, the time sequences are not always presented at the same time intervals, and only the frames that reveal new finger structures and help understand the growth mechanisms of these structures are shown. Moreover the initial system without chemical reaction is considered to be unstable, i.e.

$$\mu_A < \mu_B$$

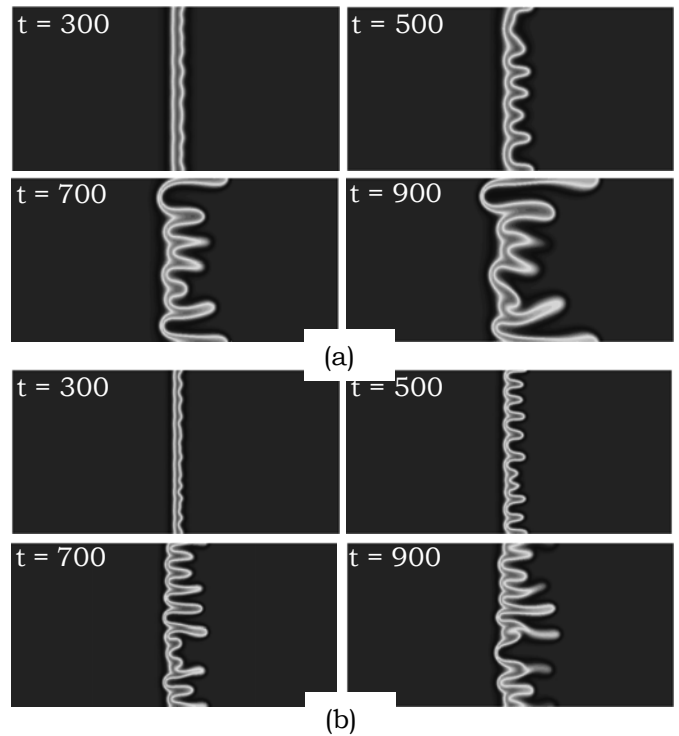


Fig 3. Concentration iso-surfaces for $Da=0.5$ $Rb=1$ $Rc=-1$: (a) $Pe=1000$ (b) $Pe=1500$

Fig.2a-b show concentration iso-surfaces of the displacing fluid for non-reactive and reactive flows. Clearly there are more fingers that tend to be narrower in the reactive case. Furthermore, the displacing front is sharper when reaction is present. Fig.2c depicts concentration of the product which is surrounded by fluids A and B, hence one can distinguish two fronts; a trailing (A-C) and a leading (C-B) front. A comparison of part b and c in Fig.2 shows that the finger structures shown in (b) are well captured by the (A-C) trailing front in (c). Therefore plots of the product concentration are a good representation of the fingering phenomena in the system and from now on only plots of the product concentration are presented.

Figs. 3 and 4 depict the effects of the Peclet number Pe and the Damkohler number Da respectively for a flow where the viscosity of the product is smaller than that of either reactants; $\mu_C < \mu_A < \mu_B$. As expected, in this case the instability is mostly developing at the leading (C-B) front while the trailing (A-C) front is virtually stable. Fig. 3 reveals that a larger number of fingers results from a larger Peclet number, however these fingers extend less in the downstream direction. It is not however clear whether a larger Peclet number results in smaller or larger chemical production. A comparison between two different Damkohler numbers in Fig. 4 reveals that the Damkohler number does not seem to have a strong effect on the fingering patterns. The only difference that one may mention is that for higher Damkohler number ($Da=0.5$) the instabilities start to grow at earlier time and the leading (C-B) front tends to be more unstable.

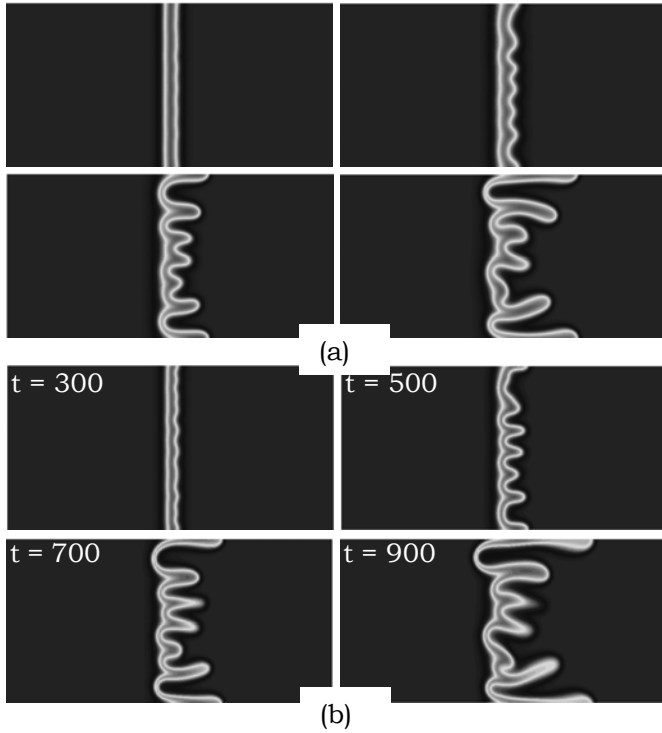


Fig 4. Concentration iso-surfaces for $A=2$, $R_b=1$, $R_c=-1$, $Pe=1000$: (a) $Da=0.1$ (b) $Da=0.5$

A quantitative analysis of the variation of the amount of chemical product with time (eq. 20) for different values of P_e and D_a has been conducted. In all the plots, the log mobility ratios are fixed as $R_b=1$, $R_c=-1$ which implies that the initial front between the reactants is unstable and that the trailing front (A-C) is stable while the leading one (C-B) is unstable. For illustrative purposes and as a reference case, we also included results for a displacement where all fronts are stable ($R_b=R_c=0$).

$$\langle C(t) \rangle = \frac{1}{LW} \int_0^L \int_0^W C(x, y, t) dy dx \quad (20)$$

Fig. 5 depicts the variation of the amount of chemical product for different values of the Peclet number and for $D_a = 0.5$. As expected, the amount of chemical product increases monotonically with time. Furthermore, it is apparent that the amount of chemical production varies as a power of time ($\propto t^n$) and that there are two regions each with a constant exponent index n . The first region is characterized by a low rate of increase while in the second one, the rate of chemical production increases fast with time. Note that the power exponent seems to be independent of P_e , at least in the first region. For the fixed Damkohler number ($D_a = 0.5$); the amount of chemical product decreases with increasing P_e . This result is counter-intuitive as larger Peclet number is usually associated with stronger instabilities and therefore more mixing between the different species. However this result may be explained by the fact that once the reaction sets in, a layer of chemical product (C) forms between the two reactants and it is speculated that the mixing between the reactants is dominated by diffusion. Therefore, larger Peclet numbers which imply a weaker diffusion result

in less mixing and as a consequence less chemical production.

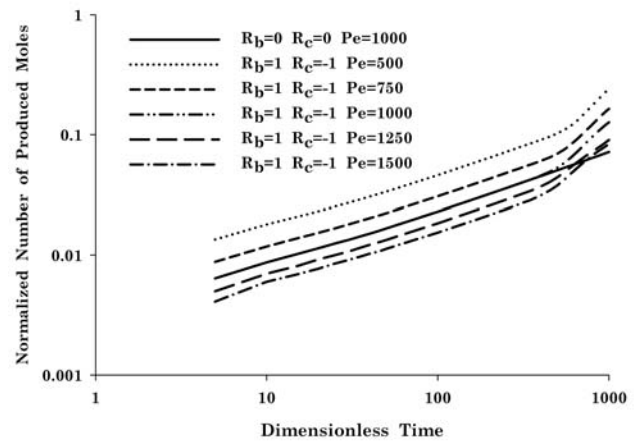


Fig 5. Normalized number of produced moles for $Da=0.5$

Changes of the amount of chemical product with time for a fixed Peclet number ($P_e = 1000$) but for different Damkohler numbers are shown in Fig.6. In this case and for the set of parameters chosen, the variation of the amount of chemical product with time seems to be less sensitive to the Damkohler number. In fact, in the first region there is an indication that the small value of Damkohler numbers leads to slightly larger amounts of the chemical product than the large D_a . In the second region, the amount of chemical product increases sharply with time and is larger for larger Damkohler numbers. Note that in this region, the power index n seems to be independent of the values of D_a .

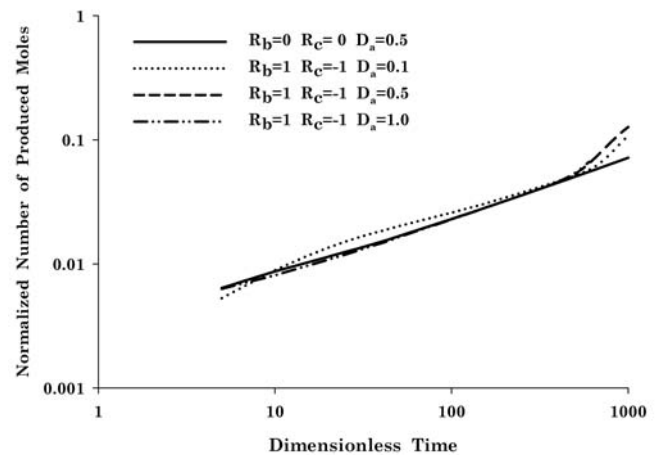


Fig 6. Normalized number of produced moles for $Pe=1000$

These trends may be explained as follows. At early times, larger D_a lead to stronger rates of production that tend to reduce the contact area between the reactants as the chemical product C fills the gap between the reactants A and B . Consequently, diffusion plays a more important role and explains the higher rate of production for small D_a . At later times, the strong instability that develops at the leading (C-B) front as a result of a larger reaction rate at large D_a , leads to stronger mixing and better contact between the two reactants.

This can be seen from frame ($t=500$) in Figure 4. In this case, narrower gaps separating the reactants are found when $Da = 0.5$ in comparison with the case $Da = 0.1$.

Few last comments regarding the reference case ($Rb=0$ $Rc=0$, $Pe=1000$, $Da=0.5$) need to be made. First, for this case where the fronts between all species are stable, the two separate regions identified earlier do not exist, and the rate of chemical product is constant throughout the whole process of displacement. Second, at large times the amount of chemical product in the reference case is less than any of the other cases where the reactants front and the leading front are unstable. Finally, for short times the reference case shows the same amount of chemical product as the case ($Rb=1$ $Rc=-1$, $Pe=1000$, $Da=0.5$), which may indicate that in the first region the amount of chemical production does not depend on the mobility ratios of the different species. This inference needs to be further examined by looking at a wider range of mobility ratios for the chemical reactants and the product.

V. CONCLUSION

The effects of different parameters on the finger structure in miscible displacements with second order chemical reaction were examined by conducting full nonlinear simulations. It was found that the efficiency of the chemical reaction which can be measured in terms of the rate of chemical product depends on two major dimensionless groups, namely the Peclet number Pe representing the ratio of convective to diffusive times and the Damkohler number Da representing the ratio of hydrodynamic to chemical times. The viscosities of the reactants and product are also expected to affect the efficiency of the chemical reaction but were not analyzed in this study

It was found that, for the range of parameters examined, larger Peclet number lead to less amounts of chemical production. This implies that diffusive effects play a more important role than convective effects, and that for practical purposes smaller injection rates should be preferred if one wants to attain higher rates of chemical production. Furthermore, the rate of the chemical reaction represented by the Damkohler number does not have strong effects on the finger structures and the development of the instability, at least in the early stages of the displacement. It was also found that changes in the Damkohler number have less effects on the efficiency of the chemical reaction than changes in the Peclet number. Finally, for large times, curves for the amount of chemical product do not change much with increase in the Damkohler number beyond a certain critical value of Da .

ACKNOWLEDGMENT

The authors acknowledge the Natural Science and Engineering Research Council of Canada (NSERC), the Alberta Ingenuity Center for In-Situ Energy (AICISE) and Alberta Ingenuity Fund (AIF) for financial support. They also thank Westgrid Research Network of Western Canada for computational resources.

REFERENCES

- [1] Saffman, P.G. and Taylor, G., The penetration of a fluid into a porous medium or Hele-Shaw cell containing a more viscous liquid, *Proc. R. Soc. Lond. A* Vol. 245, pp. 312-329 (1958).
- [2] Homsy, G.M., Viscous fingering in porous media, *Ann. Rev. Fluid Mech.* Vol. 19, pp 271-311 (1987).
- [3] McCloud, K.V. and Maher, J.V., Experimental perturbations to Saffman-Taylor flow, *Physics Reports* Vol. 260, pp. 139-185 (1995).
- [4] Islam M.N. and Azaiez, J., Fully implicit finite difference pseudo-spectral method for simulating high mobility-ratio miscible displacements, *Int. J. Num. Meth. Fluids* Vol. 47, pp. 161-183 (2005).
- [5] Carey, M.R., Morris, S.W., Kolodner, P.: Convective fingering of an autocatalytic reaction front. *Phys. Rev. E* Vol. 53, pp. 6012-6015 (1996)
- [6] Bockmann, M., Muller, S.C.: Growth rates of the buoyancy-driven instability of an autocatalytic reaction front in a narrow cell. *Phys. Rev. Lett.* Vol. 85, pp. 2506-2509 (2000)
- [7] Nagatsu, Y., Ueda, T.: Effects of reactant concentrations on reactive miscible viscous fingering. *Fluid. Mech. Trans. Phenom.* Vol. 47, pp. 1711-1720 (2001)
- [8] Horvath, D., Bansagi, T., Toth, A.: Orientation-dependent density fingering in an acidity front. *J. Chem. Phys.* Vol. 117, pp. 4399-4402 (2002)
- [9] Coroian, D.I., Vasquez, D.A.: The effect of the order of autocatalysis for reaction fronts in vertical slabs. *J. Chem. Phys.* Vol. 119, pp. 3354-3359 (2003)
- [10] Rica, T., Horvath, D., Toth, A.: Density fingering in acidity fronts: effect of viscosity. *Chem. Phys. Lett.* Vol. 408, pp. 422-425 (2005)
- [11] Zadrazil, A., Kiss, I.Z., D'Hernoncourt, J., Sevcikova, H., Merkin, J.H., De Wit, A.: Effects of constant electric fields on the buoyant stability of reaction fronts. *Phys. Rev. E* Vol. 71, 26224-1-11 (2005)
- [12] Huang, J., Edwards, B.F.: Pattern formation and evolution near autocatalytic reaction fronts in a narrow vertical slab. *Phys. Rev. E* Vol. 54, 2620-2627 (1996)
- [13] Vasquez, D.A., Wilder, J.W., Edwards, B.F.: Chemical wave propagation in Hele-Shaw cells and porous media. *J. Chem. Phys.* Vol. 104, pp. 9926-31 (1996)
- [14] De, D., Hrymak, A. N., Pelton, H.: A Network of zones model for reactive polymer enhanced miscible displacement in a porous cylinder. *Chem. Eng. Sci.* Vol. 53, pp. 3445-3559 (1998)
- [15] De Wit, A., Homsy, G.M.: Nonlinear interactions of chemical reactions and viscous fingering in porous media. *Phys. Fluids* Vol. 11, pp. 949-51 (1999)
- [16] De Wit, A., Homsy, G.M.: Viscous fingering in reaction-diffusion systems. *J. Chem. Phys.* Vol. 110, pp. 8663-75 (1999)
- [17] De Wit, A.: Fingering of chemical fronts in porous media. *Phys. Rev. Lett.* Vol. 87, 054502, pp. 1-4 (2001)
- [18] Yang, J., D'Onofrio, A., Kalliadasis, S., De Wit, A.: Rayleigh-Taylor instability of reaction-diffusion acidity fronts. *J. Chem. Phys.* Vol. 117, pp. 9395-9408 (2002)
- [19] Bansagi, T., Jr., Horvath, D., Toth, A., Yang, J., Kalliadasis, S., De Wit, A.: Density fingering of an exothermic autocatalytic reaction. *Phys. Rev. E* Vol. 68, pp. 55301-55314 (2003)
- [20] D'Hernoncourt, J., Kalliadasis, S., De Wit, A.: Fingering of exothermic reaction-diffusion fronts in Hele-Shaw cells with conducting walls. *J. Chem. Phys.* Vol. 123, pp. 234503-1-9 (2005)
- [21] Coroian, D.I., Vasquez, D.A.: The effect of the order of autocatalysis for reaction fronts in vertical slabs. *J. Chem. Phys.* Vol. 119, pp. 3354-3359 (2003)
- [22] Vasquez, Desiderio A., De Wit, A.: Dispersion relations for the convective instability of an acidity front in Hele-Shaw cells. *J. Chem. Phys.* Vol. 121, pp. 935-941 (2004)
- [23] Ghesmat, K., Azaiez, J.: Miscible displacements of reactive and anisotropic dispersive flows in porous media. *Tran. Porous Med.*, Vol. 77, pp. 489-506 (2009)
- [24] Ghesmat, K., Azaiez, J.: viscous fingering instability in porous media: effect of anisotropic velocity-dependent dispersion tensor. *Tran. Porous Med.*, Vol. 73, pp. 297-318 (2008)
- [25] Tan, C.T. and Homsy, G.M., Simulation of nonlinear viscous fingering in miscible displacement, *Phys. Fluids* Vol. 31, pp. 1330-1338 (1988).
- [26] Bracewell, R.N., The Fourier transform and its applications, McGraw Hill, New York (2000).
- [27] Singh B. and Azaiez J., Numerical simulation of viscous fingering of shear-thinning fluids, *Can. J. Chem. Eng.* Vol. 79, pp. 961-967 (2001).